Haptic Surface Exploration

Allison M. Okamura, Michael A. Costa[1], Michael L. Turner,
Christopher Richard, and Mark R. Cutkosky
Dextrous Manipulation Laboratory
Stanford, CA 94305 USA
touch@cdr.stanford.edu

Abstract: We describe research at the Stanford Dextrous Manipulation Lab centered around haptic exploration of objects with robot hands. The research areas include object acquisition and manipulation and object exploration with robot fingers to measure surface features, textures and friction. We assume that the robot is semi-autonomous; it can receive guidance or supervision from humans regarding object selection and grasp choice, but is also equipped with algorithms for autonomous fine manipulation, surface exploration and feature identification. The applications of this work include object retrieval and identification in remote or hazardous environments.

1. Introduction

Haptic exploration is an important mechanism by which humans learn about the properties of unknown objects. Through the sense of touch, we are able to learn about characteristics such as object shape, surface texture, stiffness, and temperature. Unlike vision or audition, human tactile sensing involves direct interaction with objects being explored, often through a series of "exploratory procedures" [7]. Dextrous robotic hands are being developed to emulate exploratory procedures for the applications of remote planetary exploration, undersea salvage and repair, and other hazardous environment operations.

The challenges are formidable, including object detection and grasp planning, dextrous manipulation, tactile sensor development and algorithms for surface exploration and feature identification. As a consequence, fully autonomous object acquisition and exploration are not yet practical outside of carefully controlled laboratory experiments. At the other extreme, immersive telemanipulation and tele-exploration impose demands on bandwidth of force and tactile display that are not easily achieved, especially when the robot is located remotely. Our own approach therefore follows a middle road in which the robot is guided by humans but is also capable of some autonomous manipulation, local surface exploration and feature identification. Once the object is in hand, surface properties are identified and can also be replayed to human operators.

We begin by presenting an approach in which human operators can guide the process of grasping and manipulation using an instrumented glove, with

[1]also with NASA Ames Research Center, Intelligent Mechanisms Group, MS269-3, Moffett Field, CA 94035 USA

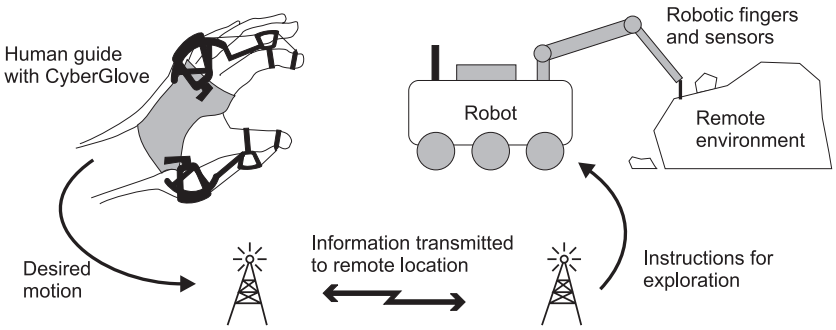

Figure 1. Guided haptic exploration of a remote surface.

or without force feedback (Figure 1). Once the object has been grasped, the robot can take over the task of surface exploration with occasional human intervention. We present several methods for detecting different surface properties. Features that are small (relative to the size of the robotic fingertip) are detected using intrinsic properties of the path traced by a spherical fingertip rolling or sliding over an object surface. Local texture profiles are recorded with a "fingernail" stylus, providing statistical measures of the surface roughness. Friction properties are estimated by measuring the relative velocities, accelerations and forces between the finger and the object during sliding. In addition, we show preliminary work on how models obtained via haptic exploration can be displayed through haptic feedback to users who may be located remotely.

2. Guiding Manipulation and Exploration

Haptic exploration requires stable manipulation and interaction with the object being explored. We are developing an approach that provides the flexibility of telemanipulation and takes advantage of developments in autonomous manipulation to reduce the required bandwidth for remote force and tactile display. A human "guide" instructs the robot through demonstration. While wearing an instrumented glove, the human reaches into a virtual environment (which may be updated with information from a real environment), grasps a virtual object and starts to manipulate it. The robot then determines the type of grasp used and the desired object motion and maps these to the kinematics of its own "hand".

There are several advantages to this approach. First, the interface is as humanly intuitive as possible and exploits the user's understanding of stable grasping and manipulation. The strategy is also flexible, because a person can quickly demonstrate a new maneuver. Meanwhile, the robot is performing the details of manipulation and force control autonomously, allowing it to optimize motions for its own capabilities and to respond immediately to information about the grasp state which it receives from its sensors. Our work indicates that when force information from the robot is displayed to the user, accurate positional resolution and force control can be achieved [17].

The most significant challenge is to obtain a best estimate of the intended

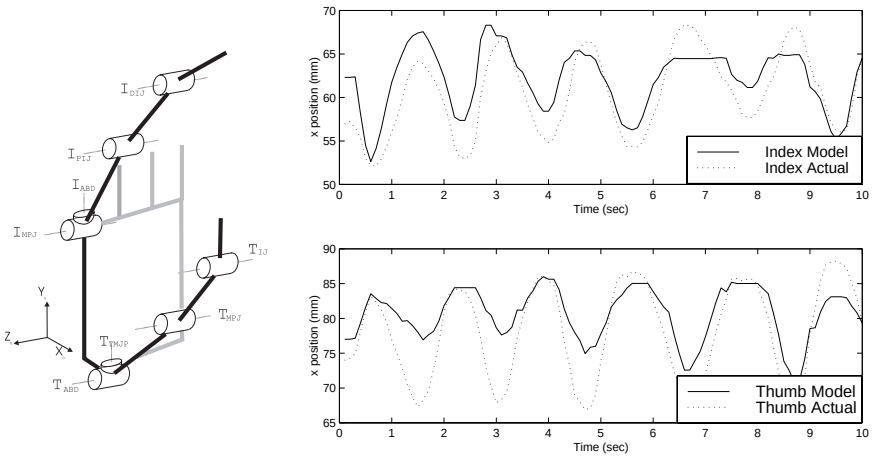

(a) (b)

Figure 2. (a) Kinematic model of the thumb and index finger. (b) Modeled and actual fingertip trajectories.

object motion. Because tactile feedback from a virtual world is imperfect at best, and possibly non-existent, the human user may make finger motions that are not consistent with a rigid object or even with stable manipulation. However, during a maneuver we can assume that the user wishes to maintain a stable grasp. For a given motion of the user's fingers, the inferred motion of the virtual object is that which minimizes the error between the virtual fingers and measurements of the user's fingers, while satisfying the kinematic constraints of rolling, sliding and maintaining the grasp.

To assist in interpreting the motion of a human hand, we have developed a kinematic model and calibration routine. The human hand model used here (Figure 2a) is an adaptation of the models developed in [14] and [8]. The joints are approximated as pure rotations, with the base joint on the thumb modeled as a spherical joint. To calibrate the manipulation, the user wears a CyberGlove from Virtual Technologies, Inc. which records the angular position of each joint while manipulating an instrumented object. Knowledge of the object position is used to infer the user's actual fingertip position. The size of the user's hand and any errors in the glove measurements are calculated with a least squares fit [14].

Six users with disparate hand sizes were used to test the calibration procedure. Reliable calibration was achieved to within an average of 4mm of measured fingertip position. Figure 2b shows a typical post-calibration comparison of thumb and index tip trajectories. Further accuracy was limited by errors in localizing the hand in space. An improved calibration device has been developed, which will be presented in future work. The CyberGlove can also be augmented with CyberGrasp, a force-reflecting exoskeleton that adds resistive force-feedback to each finger. The addition of force-feedback will be used in

future experiments with guided manipulation.

3. Surface Properties

3.1. Small Surface Features

Through guided manipulation, a robot can explore various properties of the remote environment. We consider the exploration three particular surface properties: small surface features, roughness, and friction. In this section, we present a method for detecting small surface features with a spherical robotic fingertip, with or without the use of tactile sensors. The approach can be used with guided or autonomous object exploration [13]. Although tactile sensing may be needed for control, it can be shown that surface modeling and feature detection can be accomplished without the use of tactile sensor data. We take a differential geometry approach to surface feature definition, comparing the principal curvatures of the object surface to the curvature of the fingertip.

Imagine a round fingertip rolling and sliding over the surface of an object. As the finger moves over the surface, the locus of points at the center point of the fingertip creates a parallel surface, whose principal curvatures are limited by the radius of the fingertip, r_f. For example, if the original surface has a cusp, the traced surface will have curvature $\frac{1}{r_f}$ around that point. In addition, there may be parts of the original surface that are unreachable by the fingertip, for example, a pit in the surface with radius of curvature less than $-\frac{1}{r_f}$, resulting in a discontinuity in the parallel surface. An estimate of the original surface can be calculated from the parallel surface by taking *its* parallel surface.

Features may then be extracted by comparing the curvature of either the parallel or estimated surfaces to the curvature of the fingertip. A curvature feature, as detected by a spherical robotic fingertip with radius r_f, is a region of a surface where one of the principle curvatures k_i of the surface satisfies

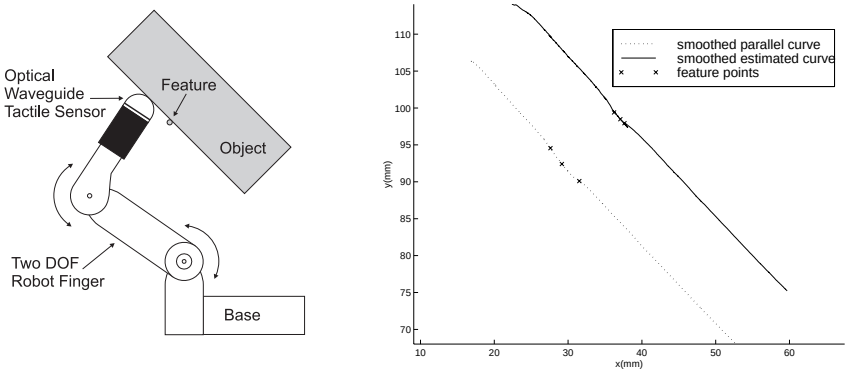

(a) (b)

Figure 3. (a) Experimental apparatus for small surface feature detection. (b) Feature detection with a robotic finger rolling/sliding on a 45° surface with a 0.65 mm bump feature.

$k_i >= \frac{1}{r_f}$ or $k_i <= -\frac{1}{r_f}$. These are the positive curvature (convex) and negative curvature (concave) features, respectively. A discontinuity on the parallel surface is especially useful for detecting negative curvature features because it is a point with infinite curvature. The simple curvature feature definition can be extended to define macro features, which consist of patterns of curvature features. For example, a bump is defined as an area following the pattern {negative curvature feature}{positive curvature feature}{negative curvature feature} as the finger travels across the surface.

Experiments in using these definitions for feature detection were performed by rolling and sliding a hemispherical fingertip over a flat surface with small ridge features. The feature was created by stretching a 0.65mm wire over the surface. The experiments were performed using two degree-of-freedom robotic fingers and 20mm diameter optical waveguide tactile sensors developed by Maekawa, et al. [9, 10] (Figure 3a). For a more detailed description of the experiments and apparatus, the reader is referred to [12].

As is typical of many robotic fingers, the workspace was limited and thus a combination of rolling and sliding was necessary to move the fingers over the surface of the object. A hybrid force/velocity control was used to obtain smooth sliding over the surface. Because the fingertip is spherical, the contact location on the finger gives the tangent and normal of the rigid surface. The velocity of the fingertip tangent to the surface and the force normal to the surface were controlled using a simple proportional law. The finger moved with an average speed of 0.03 m/sec and a normal force of 1 ± 0.01 N. Figure 3b shows the parallel and estimated surfaces and features detected for a bump on a flat surface angled at 45 degrees, with a 0.65 mm diameter wire stretched across the surface. The orientation of the object is the same as that in Figure 3a.

3.2. Surface Roughness

Below a certain scale, which depends on fingertip size and tactile sensor resolution, the perception of individual features gives way to texture. The texture of objects is an important part of their identification. Experiments with humans and robots alike have shown that the use of a "fingernail" or stylus can be a particularly effective way of characterizing textures [2]. An example application is the exploration of rock surfaces in remote planetary geology. In order to increase the sensations and science tools available to field geologists, NASA has been interested in incorporating haptics into its robotic rover field tests. Besides providing a new sensation available to geologists, it may also be possible to use haptics as a science tool to classify materials by measuring surface properties such as texture and roughness.

Surface height profiles are collected through a stylus or other sensor. In Figure 4a we compare profiles of test surface taken by a micro-machined stylus [5], Omron laser displacement sensor, and the integrated velocity signal of a phono cartridge stylus. The test surface was composed of five copper strips approximately 0.125 mm thick with adhesive backing laid onto a circuit board. While we were able to use the phono cartridge to capture the gross geometry of the test surface by integrating its velocity signal, a consistent integration error

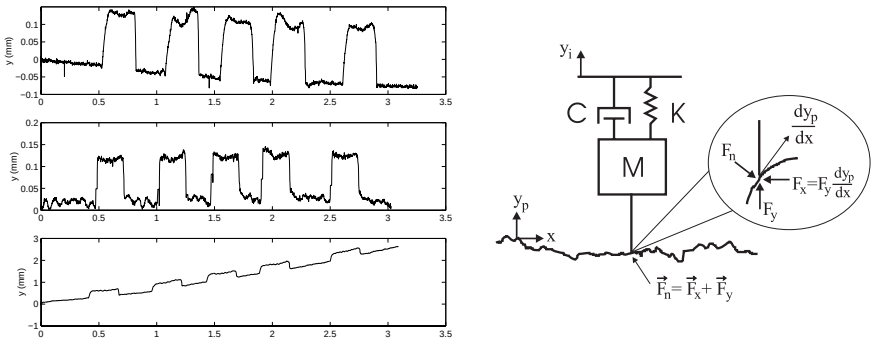

(a) (b)

Figure 4. (a) Surface profiles of flat copper strips taken by a micro-machined stylus (top), laser displacement sensor (middle), and a phono cartridge stylus (bottom). (b) Virtual stylus model.

falsely indicates a large slant in the test surface.

The collected data may subsequently be explored through a haptic interface. Using a dynamic model of stylus to surface contact, forces are displayed to a user resulting from interaction with the collected surface profile data. One such model is shown in Figure 4b. We used this model to display virtual rock surfaces to planetary geologists during a NASA Ames field experiment in February 1999.

First a height profile as a function of position, $y_p(x)$, is collected by a sensor. The stylus is then modeled as a mass, spring, damper system connected to the vertical input of the user's haptic interface device, y_i. The horizontal position of the stylus is directly coupled to the horizontal position of the interface. While in contact with the surface, the stylus dynamics are computed by the following equation.

$$M\ddot{y_p} = K(y_i - y_p) + C(\dot{y_i} - \dot{y_p}) + F_y \tag{1}$$

The constants were tuned for feel and stability to give virtual stylus parameters of $K = 0.973\frac{N}{mm}$, $C = 4.63 \times 10^{-5}\frac{N}{mm/s}$, and $M = 4.63 \times 10^{-5}g$.

The contact point of the stylus against the surface is modeled as frictionless contact point. As illustrated by the magnified portion of Figure 4b, the normal force F_n is perpendicular to the tangent at the contact point. The tangent is computed by taking the derivative of the surface with respect to the x coordinate system, $\frac{dy_p}{dx}$. In our application, this derivative is pre-computed, as we know the surface profile a priori.

The normal force is the sum of two x and y component forces. The y component represents the reaction force supporting the stylus mass from going through the virtual surface vertically. The x component represents the horizontal reaction force and is computed from the $\frac{dy_p}{dx}$ as shown in Figure 4b. While in contact with the surface, the user experiences F_x and F_y.

In practice, the lateral force F_x was scaled down to 5% of its full value. We found that using full lateral forces induced strong vibrations that detracted from the exploration of the surface. Not surprisingly, attempting to use a model with only lateral forces [11] was found to be unsatisfactory for rock surfaces. However, users who compared the models with and without lateral forces found that a small amount of lateral force improved the simulation. Interestingly, it has been claimed that surfaces modeled without friction feel glassy [4]. Although we did not use friction in this model, none of the geologists who used the system during the NASA field test or other users commented that surfaces felt glassy or slippery. We believe that a small amount of force opposing the user's horizontal motion, coupled with the irregularity of the surface, eliminates a slippery feel by creating an illusion of friction.

3.3. Friction

Although friction may not be necessary for the display of geological surfaces stroked by a hard stylus, it is an important component of the perception of surfaces in other applications. In addition, adequate levels of friction are necessary to ensure contact stability between an object and the fingers that are grasping it. Armstrong-Helouvry [1] is an overview of the issues involved in friction measurement. Shulteis, et al. [15] show how data collected from a telemanipulated robot can provide an estimate of the coefficient of friction between two blocks; one being manipulated by the robot and the other being at rest. Our own approach to the identification of friction involves force and acceleration measurements, in combination with a friction model.

The friction model used for the experiments presented below is a modified version of Karnopp's model [6]. This model includes both Coulomb and viscous friction and allows for asymmetric friction values for positive and negative velocities. It is distinct from the standard Coulomb + viscous friction model because it allows the static friction condition to exist at non-zero velocity if the magnitude of the velocity is less than a small, predefined value. The model is expressed as

$$F_{friction}(\dot{x}, F_a) = \begin{cases} C_n sgn(\dot{x}) + b_n \dot{x} & : \quad \dot{x} < -\Delta v \\ \max(D_n, F_a) & : \quad -\Delta v < \dot{x} < 0 \\ \min(D_p, F_a) & : \quad 0 < \dot{x} < \Delta v \\ C_p sgn(\dot{x}) + b_p \dot{x} & : \quad \dot{x} > \Delta v \end{cases} \tag{2}$$

where

C_p and C_n are the positive and negative values of the dynamic friction,
b_p and b_n are the positive and negative values of the viscous friction,
$\dot{x}$ is the relative velocity between the mating surfaces,
D_p and D_n are the positive and negative values of the static friction,
Δv is the value below which the velocity is considered to be zero, and
F_a is the sum of non-frictional forces being applied to the system.

A one degree-of-freedom linear motion experiment was constructed in order to conduct friction identification experiments (See Figure 5). The friction and mass of an aluminum block sliding on a sheet of rubber were estimated. The

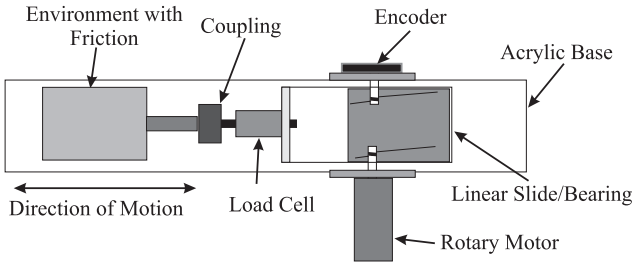

Figure 5. Schematic (top view) of the experimental apparatus.

procedure for friction identification can be summarized as follows: (1) Model the force/motion interaction of the system, (2) Move system over a range of velocities of interest, (3) Record force/motion variables included in the model, and (4) Solve for unknown parameters of the system model.

For each friction measurement experiment the aluminum block was connected to the apparatus and the apparatus was commanded to move with a periodic trajectory. Various periodic trajectories having frequencies ranging between of 0.5-3 Hz were explored. The trajectory presented here is a sinusoid with a frequency of 2 Hz and an amplitude of 0.01 meters. Trajectory amplitudes and frequency were selected to include the range of velocities for which friction estimates were desired.

The system was exercised for 10 seconds prior to collecting data for each experiment. This warm-up allowed the motion to come to steady state, and also eliminated the phenomenon of rising static friction because the system was not allowed to dwell at zero velocity for a significant period. After the 10 second warm-up was complete, the force applied to the aluminum block was recorded, along with the block's position, velocity and acceleration. Data were collected for 2 seconds, corresponding to four cycles and seven velocity reversals. The sample rate for data collection and motion control was 1 kHz.

By expressing the parameters of our model as linear coefficients of our inputs, the parameters can be estimated using least squares regression, or maximum likelihood methods. As a first step in expressing the model parameters in a linear fashion, we separate the data into two bins. One bin contains data for velocities of magnitude less than Δv. The second bin holds the remaining data. Δv is selected as the smallest velocity range that fully encompasses the transition from static to dynamic friction. After the data points corresponding to low velocities are removed, the recorded velocity vector is split into two new velocity vectors. The velocity vector vel_p is equal to the original vector vel except that negative velocity values are replaced with zeros. The velocity vector vel_n contains the negative portion of the original velocity vector and has zeros where there are positive values in vel.

Now, the measured force can be expressed as the sum of the inertia force, and the friction as

$$F_m = X\beta + \epsilon \tag{3}$$

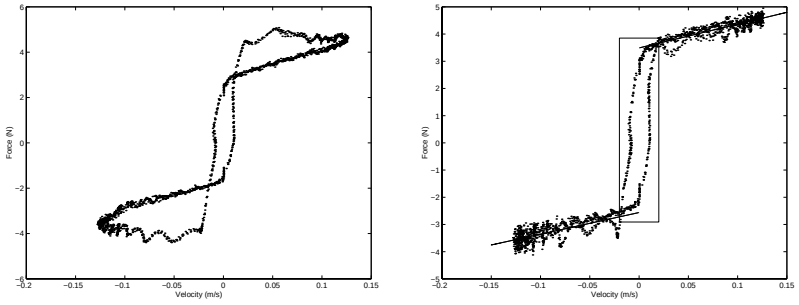

(a) (b)

Figure 6. (a) Measured force versus velocity for aluminum on rubber (four motion cycles). (b) Measured force adjusted for mass and model of estimated friction for aluminum on rubber.

where

F_m is the measured force,
X is a matrix of measured accelerations and velocities,
β is a vector of friction model parameters $[m, C_p, b_p, C_n, b_n]^T$, and
ϵ is the measurement error.

Least squares regression assumes that the measured variables, acceleration and velocity in our case, are free of measurement error. Fuller[3] presents several alternate estimators that account for errors in the input variables and provide unbiased estimates of β. Assuming that the errors in each of our measured variables are independent of each other, β is estimated as

$$\tilde{\beta} = \left(N^{-1}X^TX - \ddot{S}_{uu}\right)^{-1}\left(N^{-1}X^TF_m\right) \tag{4}$$

where N is the number of samples,
$\ddot{S}_{uu} = diag(s_{\delta a}, 0, s_{\delta vel}, 0, s_{\delta vel})$,
$s_{\delta a}$ is the estimated variance of the acceleration error, and
$s_{\delta vel}$ is the estimated variance of the velocity error.

A friction estimate was obtained by using the method outlined to identify the friction and mass of an aluminum block sliding on rubber. The mass of the block was presumed unknown for each experiment; however, for verification purposes the block was weighed and found to be 0.419kg. Figure 6a shows the typical raw force data plotted against velocity. The effects of stick-slip vibration are evident. Figure 6b shows the raw force adjusted for the estimated mass. The solid lines in Figure 6b represent the predicted friction using the parameters in Equation 2. The rectangular box shows Δv, D_n and D_p.

4. Conclusion and Future Work

In this work, we have outlined an approach for guided manipulation and haptic exploration using an instrumented glove, and presented various exploratory procedures utilizing different types of sensors.

In each of the sensing approaches, there is considerable future work in the development and refinement of detection schemes and haptic display algorithms to play back surface properties. At present, the different sensing methods have been individually tested; the eventual goal is to create an integrated system capable of using many different sensors and exploratory procedures. Further experiments in guided manipulation and haptic exploration are underway with a pair of two degree-of-freedom robotic fingers mounted on an Adept robot.

References

[1] B. Armstrong-Helouvry, *Control of Machines with Friction*, Kluwer Academic Publishers, Norwell, MA, 1991.

[2] G. Buttazzo, et al., "Finger Based Exlorations," *Proceedings of SPIE - The International Society for Optical Enigneers*, Vol. 726, pp. 338-345, 1986.

[3] W. Fuller, *Measurement Error Models*, John Wiley and Sons, New York, 1987.

[4] D.F. Green, "Texture Sensing and Simulation Using the PHANToM: Towards Remote Sensing of Soil Porperties," *Second PHANToM User's Group Workshop*, Oct. 19-22, 1997.

[5] B. Kane, et al., "Force-Sensing Microprobe for Precise Stimulation of Mechanosensitive Tissues," *IEEE Trans. on Biomedical Engineering*, Vol. 42, No. 8, pp. 745-750, 1995.

[6] D. Karnopp, "Computer simulation of stick-slip friction in mechanical dynamic systems," *ASME Journal of Dynamic Systems, Measurement and Control*, Vol. 107, pp. 100-103, 1985.

[7] R. Klatzky and S. Lederman, "Intelligent Exploration by the Human Hand," Chapter 4, *Dextrous Robot Manipulation*, Springer-Verlag, 1990.

[8] J. Kramer, "Determination of Thumb Position Using Measurements of Abduction and Rotation," US Patent #5,482,056, 1996.

[9] H. Maekawa, et al., "Development of a Three-Fingered Robot Hand with Stiffness Control Capability," *Mechatronics*, Vol. 2, No. 5, pp. 483-494, 1992.

[10] H. Maekawa, et al., "A Finger-Shaped Tactile Sensor Using an Optical Waveguide," *IEEE Intl. Conf. on Systems, Man and Cybernetics*, pp. 403-408, 1993.

[11] M. Minsky, et al., "Feeling and Seeing: Issues in Force Display," *Computer Graphics (ACM)*, Vol. 24, No. 2, pp. 235-243.

[12] A. Okamura and M. Cutkosky, "Haptic Exploration of Fine Surface Features," *IEEE Intl. Conf. on Robotics and Automation*, in press, 1999.

[13] A. Okamura, et al., "Haptic Exploration of Objects with Rolling and Sliding," *IEEE Intl. Conf. on Robotics and Automation*, pp. 2485-2490, 1997.

[14] R. Rohling and J. Hollerbach "Calibrating the Human Hand for Haptic Interfaces," *Presence: Teleoperators and Virtual Environments*, Vol. 2, No. 4, pp. 281-296, 1993.

[15] T. Schulteis, et al., "Automatic Identification of Remote Environments," *Proc. of the ASME Dynamic Systems and Control Division*, Vol. 58, pp. 451-458, 1996.

[16] M. Tremblay and M. Cutkosky, "Estimating friction using incident slip sensing during a manipulation task," *IEEE Intl. Conf. on Robotics and Automation*, pp. 429-434, 1993.

[17] M. Turner, et al., "Preliminary Tests of an Arm-Grounded Haptic Feedback Device in Telemanipulation," *Proc. of the ASME Dynamic Systems and Control Division*, Vol. 64, pp. 145-149, 1998.